

Mean Field Theory of Polynuclear Surface Growth

E. Ben-Naim¹, A. R. Bishop¹, I. Daruka^{1,2}, and P. L. Krapivsky³

¹*Theoretical Division and Center for Nonlinear Studies, Los Alamos National Laboratory, Los Alamos, NM 87545*

²*Department of Physics, University of Notre Dame, Notre Dame, IN 46556*

³*Center for Polymer Studies and Department of Physics, Boston University, Boston, MA 02215*

We study statistical properties of a continuum model of polynuclear surface growth on an infinite substrate. We develop a self-consistent mean-field theory which is solved to deduce the growth velocity and the extremal behavior of the coverage. Numerical simulations show that this theory gives an improved approximation for the coverage compare to the previous linear recursion relations approach. Furthermore, these two approximations provide useful upper and lower bounds for a number of characteristics including the coverage, growth velocity, and the roughness exponent.

PACS numbers: 02.50.Ey, 05.40.+j, 82.20.Mj, 82.60.Nh

I. INTRODUCTION

Kinetics of surface growth is a fascinating field that has been the subject of intense current research [1–4]. It is well established that as the surface grows its morphology remains scale invariant, and for example, fluctuations in the interface height exhibit an asymptotic scaling behavior. While the understanding of growth on one-dimensional (1d) substrates is rather comprehensive, in the physical case of two-dimensional substrates current theoretical understanding remains incomplete [3,4].

In this study we focus on an appealingly simple yet non-trivial surface growth problem, the so-called polynuclear growth (PNG) model [5–7]. The PNG model describes the evolution of islands that nucleate at random on top of previously nucleated islands and grow in the radial direction. This model is appropriate for describing situations where there is a competition between growth along the step edges and growth due to nucleation, as is the case in polymer crystal growth [8,9].

The submonolayer version of the PNG model is identical to the classical Kolmogorov-Avrami-Johnson-Mehl (KAJM) nucleation-and-growth process [10–12] where exact results for the coverage and more detailed statistical properties are possible [13–16]. Using the exact solution for the KAJM coverage, an approximate Linear Recursion Relations (LRR) approach to the PNG process in arbitrary dimension was suggested [6,17–19]. Additionally, steady states on 1d substrates were obtained analytically using the fact that kinks (antikinks) are uncorrelated [5,20,21]. However, the non-equilibrium behavior and especially the asymptotic time dependence remains an open problem, despite a number of studies [18–24].

Our goal is to develop a self-consistent approach that can be viewed as a mean field theory (MFT) of the PNG process, and to compare it with the previous LRR approximation as well as with numerical simulations. We will show that MFT offers a better description for the time dependent coverage, and that the two approaches, when combined, provide upper and lower bounds for the coverage and the growth velocity.

The rest of this paper is organized as follows. In the

next section we define the PNG model. In Sec. III, we develop a self-consistent mean field approximation. We find that possible growth velocities are bounded from below, $v \geq v_{\min}$, and show that the minimal velocity is actually selected. We also solve for the coverage profile in the tail regions. In Sec. IV, we review the LRR approach and derive the coverage profile analytically. In Sec. V, we present simulation results. Conclusions are given in Sec. VI.

II. THE PNG MODEL

The PNG model is defined as follows. Consider a flat uniform d -dimensional substrate at time $t = 0$. Seeds of negligible size nucleate randomly at a constant rate per unit area, and grow with a constant velocity in the radial direction. When two islands on the same layer meet they coalesce, and the joint perimeter continues growing in the corresponding radial direction. Meanwhile, nucleation continuously generates additional layers on top of previously nucleated layers. Clearly, there are no overhangs in this model, a feature that considerably simplifies the analysis. Another important simplification in the PNG model is that the nucleation rate is uniform in time as well as in space, i.e., it is independent of the local surface structure. Without loss of generality, we set the nucleation rate and the radial growth velocity to unity. This can be achieved by an appropriate rescaling of space and time.

In this study, we concentrate on $S_j(t)$, the uncovered fraction in the j th layer at time t . This important characteristic of multilayer growth gives the net exposed fraction of the j th layer, $S_j(t) - S_{j-1}(t)$, and therefore can be used to calculate relevant statistical properties. In general $\langle f(j) \rangle = \sum_{j=0}^{\infty} f(j)[S_{j+1}(t) - S_j(t)]$, and in particular the average height is given by

$$h(t) = \langle j \rangle = \sum_{j=1}^{\infty} j [S_{j+1}(t) - S_j(t)]. \quad (1)$$

Fluctuations in the height are quantified by the mean square width or roughness, $w^2(t)$,

$$\begin{aligned}
w^2(t) &= \langle j^2 \rangle - \langle j \rangle^2 \\
&= \sum_{j=1}^{\infty} j^2 [S_{j+1}(t) - S_j(t)] - h^2(t).
\end{aligned}
\tag{2}$$

We expect a linear growth in time for the average height, $h(t) \simeq vt$, and an algebraic growth for the interface width, $w(t) \sim t^\beta$, with a priori unknown roughness exponent β . In other words, the uncovered fraction obeys the following wave-like form

$$S_j(t) = F\left(\frac{j - vt}{t^\beta}\right). \tag{3}$$

The argument reflects the overall shift in the position of the wave-front, and the multiplicative scale accounts for the algebraic widening of the front.

Far from the front region, we anticipate the following extremal behavior of the scaling function $F(z)$:

$$F(z) \sim \begin{cases} 1 - \exp(-z^{\sigma_+}) & z \rightarrow \infty; \\ \exp(-|z|^{\sigma_-}) & z \rightarrow -\infty. \end{cases} \tag{4}$$

The exponents σ_\pm thus characterize relaxation away from the front region. The exponent σ_+ which describes large positive fluctuations in the height can be simply related to the roughness exponent. Consider a large positive height fluctuation, $j = Avt$, with $A \gg 1$. Such large ‘‘towers’’ can be created only by an anomalously large number, Avt , of nucleation events localized in the same region. Given the Poisson nature of the nucleation events, such fluctuations are suppressed exponentially. Thus, the quantity $1 - S_{Avt}(t)$ is estimated by $\exp(-t)$, but since Eq. (4) gives $\exp[-t^{\sigma_+(1-\beta)}]$, we conclude that

$$\sigma_+ = \frac{1}{1-\beta}. \tag{5}$$

III. MEAN FIELD THEORY

In the following, we explore the *non-equilibrium* regime, i.e., we consider polynuclear growth on an infinite substrate. Non-equilibrium behavior should agree with the early time behavior on finite substrates, since then finite size effects are still negligible.

A. One Dimension

We start with the PNG model in one dimension where a more comprehensive analysis is possible. In this situation, steps nucleate in pairs and move away from each other with a constant velocity. The constant nucleation rate and the growth velocity are set to unity, without loss of generality. Hence, the length of an island at time t after birth equals $2t$. Consider $f_j(x, t)$, the density of gaps

of length x at time t in the j th layer. This distribution evolves according to

$$\begin{aligned}
\frac{\partial f_j(x, t)}{\partial t} &= 2 \frac{\partial f_j(x, t)}{\partial x} \\
&+ \gamma_j(t) \left[-x f_j(x, t) + 2 \int_x^\infty dy f_j(y, t) \right].
\end{aligned}
\tag{6}$$

The spatial derivative term describes shrinkage of gaps. The last two terms account for changes due to nucleation and thus, are proportional to the overall nucleation rate at the j th layer, $\gamma_j(t)$. The loss term is proportional to the gap length and the gain term describes creation of gaps from larger gaps.

Eqs. (6) contain yet unknown nucleation rates $\gamma_j(t)$ which will be chosen to satisfy the correct kinetic equations for the uncovered fractions

$$S_j(t) = \int_0^\infty dx x f_j(x, t), \tag{7}$$

and the gap (or island) densities

$$N_j(t) = \int_0^\infty dx f_j(x, t). \tag{8}$$

The uncovered fraction decreases with a rate proportional to the island density, $\dot{S}_j(t) = -2N_j(t)$, and by integrating Eqs. (6) we indeed recover this exact equation. The island density changes due to disappearance of gaps as well as due to nucleation. The total nucleation rate is proportional to the exposed fraction of the j th layer and thus, $\dot{N}_j(t) = -2f_j(0, t) + S_j(t) - S_{j-1}(t)$. On the other hand, by integrating Eqs. (6) we obtain $\dot{N}_j(t) = -2f_j(0, t) + \gamma_j(t)S_j(t)$. Therefore, the choice

$$\gamma_j(t) = 1 - \frac{S_{j-1}(t)}{S_j(t)} \tag{9}$$

guarantees that the gap density evolves according to *exact* rate equation. The expression of Eq. (9) for the nucleation rate $\gamma_j(t)$ in the j th layer is intuitively appealing since the total unit nucleation rate should be reduced to account for nucleation events below the j th layer. Taking into account that $S_0(t) \equiv 0$ we find $\gamma_1(t) \equiv 1$ and we notice that Eq. (6) for the first layer agrees with the exact KAJM equation [13]. Thus, the set of rate equations (6) with the nucleation rates (9) provides a self-consistent description of the 1d PNG model. It is exact for the first layer, and additionally, the first two moments of the gap density satisfy the correct rate equations. However, it is a mean-field description since it assumes a spatially homogeneous nucleation rate $\gamma_j(t)$.

The gap density is found to be exponential, and the formal solution reads

$$f_j(x, t) = g_j^2(t) \exp\left[-g_j(t)x - 2 \int_0^t d\tau g_j(\tau)\right], \tag{10}$$

with $g_j(t) = \int_0^t d\tau \gamma_j(\tau)$. The uncovered fraction and the island density are evaluated using Eqs. (7) and (8):

$$\begin{aligned} S_j(t) &= e^{-2 \int_0^t d\tau g_j(\tau)}, \\ N_j(t) &= g_j(t) S_j(t). \end{aligned} \quad (11)$$

Evaluating $d^2 \ln S_j(t)/dt^2$ together with Eq. (9) and $\dot{g}_j(t) = \gamma_j(t)$, leads to an infinite set of recursive differential equations for the uncovered fraction

$$\ddot{S}_j - \dot{S}_j^2 S_j^{-1} + 2(S_j - S_{j-1}) = 0. \quad (12)$$

Eqs. (12) should be solved subject to the initial conditions $S_j(0) = 1$ and $\dot{S}_j(0) = 0$ for $j \geq 1$. The recursive structure of Eqs. (12) reflects the fact that kinetics of a given layer is *unrelated* to that of all layers above (thanks to the absence of overhangs). Additionally, Eqs. (12) agree with the nature of the PNG model implying that kinetics of a given layer should be *directly* coupled only to the previous layer.

Using $S_0(t) \equiv 0$, $S_1(t)$ is determined, then $S_2(t)$, etc. Of course, for the first layer, the KAJM nucleation-and-growth results are reproduced [13]

$$\begin{aligned} S_1(t) &= e^{-t^2}, \\ f_1(x, t) &= t^2 e^{-xt - t^2}. \end{aligned} \quad (13)$$

It is also possible to solve analytically for the second layer

$$\begin{aligned} S_2(t) &= \cosh^2 t e^{-t^2}, \\ f_2(x, t) &= [t \cosh t - \sinh t]^2 e^{-(t - \tanh t)x - t^2}. \end{aligned} \quad (14)$$

Using the transformation, $S_j(t) = \exp[u_j(t) - t^2]$, the differential equations (12) formally simplify to a directed version of the Toda equations [25], $\ddot{u}_j = 2 \exp[u_{j-1} - u_j]$, with the initial conditions $u_j(0) = \dot{u}_j(0) = 0$ and the boundary condition $u_1(t) = 0$. Despite this simplification it is not possible to integrate these equations, and we solve numerically for $S_j(t)$. Fig. 1 shows how the coverage in a given layer changes with time. We see that the coverage quickly relaxes onto a traveling wave form with a finite width, $S_j(t) \rightarrow F(j - vt)$.

Some quantitative characteristics of the traveling wave can be determined analytically. For $j - vt \gg 1$, the non-linear term in (12) is negligible and Eqs. (12) become linear. Thus, we write

$$1 - S_j(t) \sim e^{-\alpha(j-vt)}, \quad j - vt \gg 1, \quad (15)$$

with a yet unknown coefficient α . Substituting into Eqs. (12) gives

$$v^2 = 2 \frac{e^\alpha - 1}{\alpha^2}. \quad (16)$$

The right hand side has a minimum at $\alpha = 1.59362$. Therefore any velocity in the interval $[v_{\min}, \infty)$ with $v_{\min} = 1.75735$ is possible. Our numerical integration shows a velocity that falls within 0.1% of v_{\min} , thereby implying that the minimal velocity is indeed selected.

Such minimum velocity selection is ubiquitous and occurs for a wide class of initial conditions [26,27].

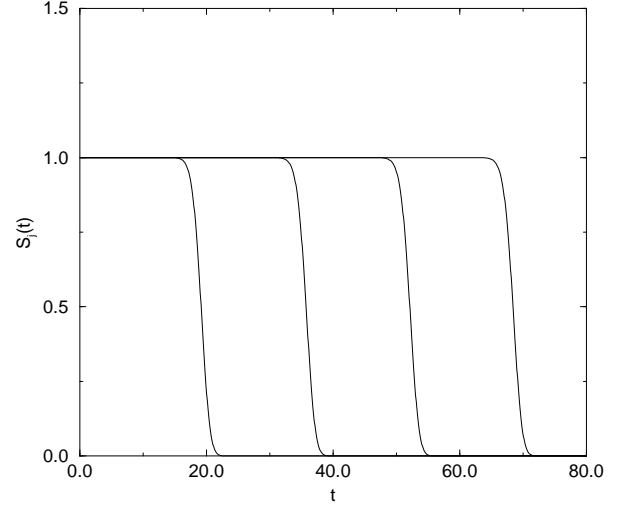


Fig.1 The uncovered fraction $S_j(t)$ vs. time for layers $j = 20, 40, 60,$ and 80 . Clearly, the coverage follows a traveling wave form.

To obtain the asymptotic behavior in the other extreme, $z = j - vt \rightarrow -\infty$, we first note that $S_2(t) \gg S_1(t)$, as follows from (13) and (14). We assume this for all layers far behind the front; we will check this assumption $S_j(t) \gg S_{j-1}(t)$ a posteriori. This reduces Eqs. (12) to $\ddot{S}_j - \dot{S}_j^2 S_j^{-1} + 2S_j = 0$ which is solved to yield $S_j(t) = \exp(-t^2 + A_j t + B_j)$. The traveling wave form implies that $S_j(t)$ should be a function of a single variable $z = j - vt$. This determines the constants A_j and B_j , and we find $S_j(t) = F(z) \sim \exp(-z^2/v^2)$. One can verify that the assumption $S_j(t) \gg S_{j-1}(t)$ is valid.

B. Arbitrary Dimension

The above analysis cannot be generalized in a straightforward manner to $d \neq 1$ since the gap distribution is intrinsically one-dimensional. However, it is still possible to obtain a mean field description for the uncovered fraction.

Consider first a KAJM nucleation-and-growth process where the rate of nucleation events $\gamma(t)$ is homogeneous in space but time dependent. Ignoring overlap between growing disks, the uncovered fraction $S(t)$ decreases with time according to

$$\frac{dS(t)}{dt} = -d\Omega_d \int_0^t d\tau \gamma(\tau) (t - \tau)^{d-1}, \quad (17)$$

where $\Omega_d = \pi^{d/2}/\Gamma(1 + d/2)$ is the volume of the d -dimensional unit sphere and $d\Omega_d$ is its surface area [28] (Γ is the gamma function). Of course, Eq. (17) overestimates the decay rate since some of the area is already

covered. Nevertheless, this may be corrected if $(-dS/dt)$ is reduced by the uncovered fraction, S ,

$$\frac{dS(t)}{dt} = -d\Omega_d S(t) \int_0^t d\tau \gamma(\tau)(t-\tau)^{d-1}. \quad (18)$$

For a constant nucleation rate, $\gamma = 1$, Eq. (18) gives

$$S(t) = \exp \left[-\frac{\Omega_d t^{d+1}}{d+1} \right]. \quad (19)$$

Thus, the exact KAJM coverage is recovered. Furthermore, a generalization of the KAJM solution to time-dependent nucleation rates appears to be equivalent to Eq. (18) [14].

We now return to the PNG model. Note first that the nonlocal in time integro-differential Eq. (18) can be converted to a higher order ordinary differential equation $d^{d+1} \ln S_j(t)/dt^{d+1} = -d! \Omega_d \gamma_j(t)$. Unlike the 1d case, it is not possible to derive the nucleation rate self-consistently. However, assuming a spatially homogeneous nucleation rate [7] implies the total nucleation rate $\gamma_j(t)S_j(t) = S_j(t) - S_{j-1}(t)$ and therefore Eq. (9). We thus arrive at the following generalization of the mean-field Eq. (12) for the uncovered fraction

$$\frac{d^{d+1}}{dt^{d+1}} \ln S_j + d! \Omega_d \left[1 - \frac{S_{j-1}(t)}{S_j(t)} \right] = 0. \quad (20)$$

The analysis presented in the one-dimensional case applies for arbitrary dimensions. For example, the transformation $S_j(t) = \exp [u_j(t) - \Omega_d t^{d+1}/(d+1)]$ reduces Eqs. (20) to a set of generalized directed Toda equations $d^{d+1} u_j/dt^{d+1} = d! \Omega_d \exp [u_{j-1} - u_j]$. Analysis of these equations or Eqs. (20) reveals that the coverage relaxes to a traveling wave with a finite width. To determine the growth velocity, we insert the ansatz of Eq. (15) into Eqs. (20) to find

$$v^{d+1} = d! \Omega_d \frac{e^\alpha - 1}{\alpha^{d+1}}. \quad (21)$$

This provides the lower bound for the growth velocity, $v_d \geq v_d^{\min}$. Again the minimal velocity should be selected, and for example $v_0 = 1$, $v_1 = 1.75735$, $v_2 = 1.67115$, and $v_d \simeq \sqrt{2\pi e/d}$ when $d \rightarrow \infty$. Furthermore, in finite dimensions mean field theory predicts universal exponents $\beta = 0$, $\sigma_+ = 1$, and $\sigma_- = 2$. (Note that the relationship of Eq. (5) is obeyed).

In the zero-dimension limit, the behavior changes qualitatively. Indeed, for the $d = 0$ case Eqs. (20) become *linear*,

$$\frac{dS_j}{dt} + S_j = S_{j-1}. \quad (22)$$

Solving (22) recursively yields the uncovered fraction, $S_j(t) = e^{-t} \sum_{i=0}^{j-1} t^i/i!$. Alternatively, by treating the variable j as continuous, this set of linear equations reduces to a simple convection-diffusion equation with a unit velocity and a diffusion coefficient $D = 1/2$. Consequently, the roughness becomes diffusive, i.e., $\beta = 1/2$.

IV. LINEAR RECURSION RELATIONS

The Linear Recursion Relations (LRR) approach employs the exact uncovered fraction $S_1(t)$ in the first layer, provided by the KAJM solution (19) [6,18,29,30]. Nucleation in the $(j+1)$ st layer proceeds only on the already covered fraction of the j th layer, formed with rate $-dS_j/dt$. Subsequent covering proceeds as in the KAJM, so one anticipates that nucleation events in the time interval $(\tau, \tau + d\tau)$ make a contribution $S_1(t - \tau) [-\dot{S}_j(\tau)] d\tau$ to the exposed fraction $S_{j+1}(t) - S_j(t)$ in the $(j+1)$ st layer. This leads to a recursion relation between adjacent layers:

$$S_{j+1}(t) = S_j(t) - \int_0^t d\tau S_1(t - \tau) \frac{dS_j(\tau)}{d\tau}. \quad (23)$$

The first layer coverage (19) can be recovered by setting the substrate coverage appropriately, $dS_0/dt = -\delta(t)$.

Although MFT and LRR are both recursive as every layer is coupled to the preceding layer, they differ in that the MFT equations are nonlinear, while the LRR equations are linear. Nevertheless, when $d \rightarrow 0$, both approximations are identical. Indeed, multiplying Eq. (23) by e^t and differentiating, one recovers the MFT equation (22).

Using the Laplace transform, analytical results for the growth velocity and the interface width have been established [30,18,19]. Below, we give an alternative and simpler derivation which additionally provides the asymptotic behavior of the coverage profile. In the long time limit, it is reasonable to treat the layer number j as a continuous variable. Replacing the difference $S_{j+1} - S_j$ by a partial derivative, the recursive relations (23) become

$$\begin{aligned} \frac{\partial S}{\partial j} &\simeq - \int_0^t d\tau S_1(\tau) \frac{\partial S(j, t')}{\partial t'} \Big|_{t'=t-\tau} \\ &\simeq - \frac{1}{v_d} \frac{\partial S}{\partial t} + \frac{1}{2v_d^2} \frac{\Gamma\left(\frac{d+3}{d+1}\right)}{\Gamma^2\left(\frac{d+2}{d+1}\right)} \frac{\partial^2 S}{\partial t^2}, \end{aligned} \quad (24)$$

with v_d the growth velocity

$$v_d = \left(\frac{\Omega_d}{d+1} \right)^{\frac{1}{d+1}} / \Gamma\left(\frac{d+2}{d+1}\right). \quad (25)$$

The second line in (24) has been derived by expanding $S(j, t - \tau)$ in a Taylor series in τ , keeping only the two dominant terms of the expansion, and replacing the upper limit in the integral by ∞ . The following growth velocities are found: $v_0 = 1$, $v_1 = 2/\sqrt{\pi} = 1.12838$, $v_2 = 1.13719$, and $v_d \rightarrow \sqrt{2\pi e/d}$ as $d \rightarrow \infty$. The velocity is almost constant for physical dimensions (it varies

by less than 4% in the range $1 \leq d \leq 4$) indicating the weak dimension dependence of this approach.

Changing variables from (j, t) to $(j, \xi = j - v_d t)$ recasts Eq. (24) into a diffusion equation

$$\frac{\partial S}{\partial t} = D \frac{\partial^2 S}{\partial \xi^2}. \quad (26)$$

The constant $D = \frac{v_d}{2} \Gamma\left(\frac{d+3}{d+1}\right) / \Gamma^2\left(\frac{d+2}{d+1}\right)$ plays the role of a diffusion coefficient and controls the width of the interface. In obtaining Eq. (26), j was replaced by $v_d t$. This is clearly valid in the scaling limit, $j \rightarrow \infty$, $|\xi| \rightarrow \infty$, $j \sim \xi^2$. The initial profile of the uncovered fraction, $S(j, 0)$, is a step function: $S(j, 0) = 0$ for $j \leq 0$ and $S(j, 0) = 1$ for $j > 0$. Solving (26) subject to these initial conditions yields

$$S(j, t) = \frac{1}{2} \text{Erfc}(-z), \quad z = \frac{\xi}{\sqrt{4Dt}} = \frac{j - v_d t}{\sqrt{4Dt}}, \quad (27)$$

with $\text{Erfc}(z) = \frac{2}{\sqrt{\pi}} \int_z^\infty du e^{-u^2}$ the error function [28]. While the two approximations generally differ in their asymptotic behavior, they do agree in the extreme cases of $d = 0$ and $d = \infty$.

In summary, the LRR approach predicts a dimension-independent “diffusive” width exponent $\beta = 1/2$. The shape of the coverage profile is symmetric and Gaussian far from the front, $\sigma_\pm = 2$.

V. COMPARISON WITH SIMULATIONS

To test the two approximations we simulated the PNG process. The simulation results presented below are for a one-dimensional chain of length $L = 10^4$ and represent a single realization. This study is different than previous numerical studies which simulated the PNG process on a lattice [24]. Here we treated time and space as continuous variables, and this enables comparison with the above theories.

The time dependence of the uncovered fraction for the first four layers is shown in Fig. 2. It is seen that the MFT and the LRR approaches provide upper and lower bounds, respectively, for the actual PNG coverage. Additionally, the MFT provides a better approximation for the uncovered fraction, $S_j(t)$. For early times, the height and width predicted by either approximations are quite close to simulation results, as shown in Fig. 3. In fact, both approaches agree to the first significant order in time, as both Eq. (12) and Eq. (23) predict $S_j(t) = 1 - \frac{2^j}{(2j)!} t^{2j}$. The disagreement between the two is of the order t^{2j+2} . As the two approximations give upper and lower bounds for the PNG process, we conclude that this is the leading early time behavior of $S_j(t)$.

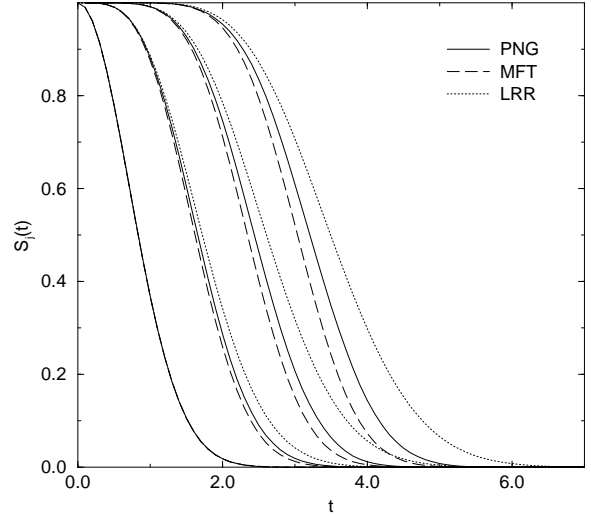


Fig. 2. Uncovered fraction $S_j(t)$ versus t for $j = 1, 2, 3, 4$. MFT and LRR approaches give lower and upper bounds, respectively, for the uncovered fraction.

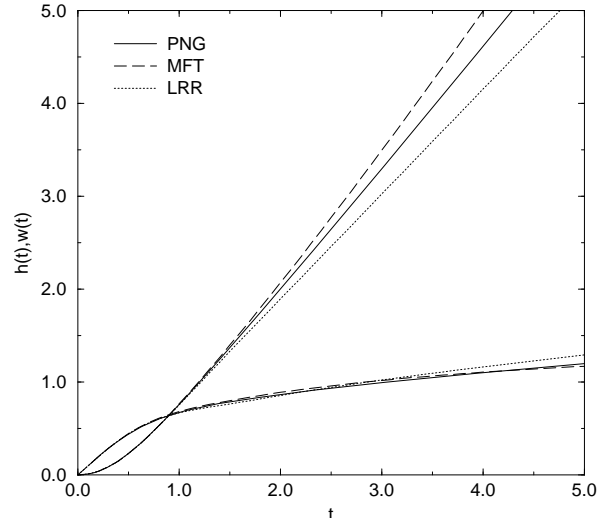


Fig. 3. Short time behavior of the height $h(t)$ and the width $w(t)$. MFT is closer to the actual behavior.

However, both approximations become progressively worse at later times. This is due to the fact that the asymptotic behavior of the width is predicted incorrectly (see Table 1). Fig. 4 shows that at least in one dimension, the PNG asymptotic behavior belongs to the KPZ universality class. As our simulations are continuous in space and time, they enable measurement of the surface growth velocity. Although in principle, there is no reason to expect that the surface growth velocity in an infinite and a finite system are equal, the numerical velocity $v_{\text{noneq}} = 1.41 \pm 0.01$, which corresponds to (non-equilibrium) growth on an infinite substrate, is in very good agreement with the known analytical equilibrium growth velocity $v_{\text{eq}} = \sqrt{2}$ [20]. Numerical values for v ,

β and σ_{\pm} are summarized in Table 1. Two-dimensional simulations give a velocity $v_2 \approx 1.4$ [7] compare to the values $v_2 = 1.671$ (MFT) and $v_2 = 1.137$ (LRR). This suggests that MFT improves for higher dimensions. Furthermore, the exponent β decreases with the dimension and it vanishes for $d \geq 4$ [3]. Above this critical dimension, mean-field behavior occurs.

We also examined the extremal behavior of $S_j(t)$ using the simulations. The scaling prediction (5) holds as the simulation data is consistent with the exponent value $\sigma_+ = 3/2$. Given that the PNG uncovered fraction is bounded by the two approximations, the parameters v , β , and therefore σ_+ are similarly bounded (see Table 1.) Since the scaling argument involves the width, one can not conclude a priori that the same holds for σ_- . Nevertheless, the exponent found in the simulation is quite close to 2, or possibly slightly larger.

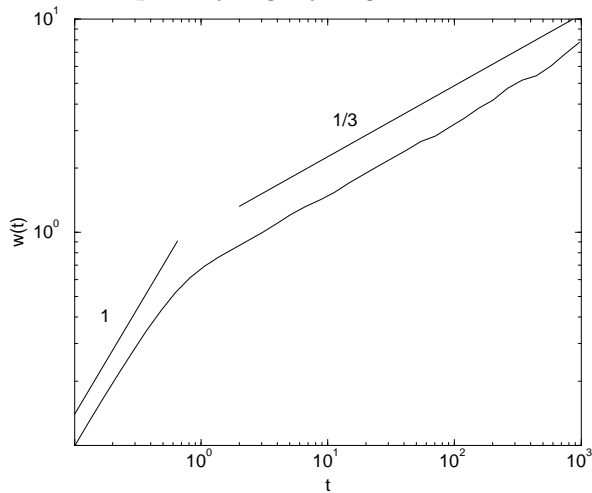


Fig.4 Long time behavior of the width. Early behavior is linear and late behavior is in the KPZ universality class $t^{1/3}$.

	MFT	PNG	LRR
v_1	1.75735	1.41 ± 0.01	1.12838
β	0	1/3	1/2
σ_+	1	3/2	2
σ_-	2	≥ 2	2

Table 1: Characteristics of the three approaches for the one-dimensional PNG model.

VI. CONCLUSIONS

We have investigated a continuum model of multilayer growth, the PNG model. We confirmed that the LRR approximation implies a dimension-independent asymptotic behavior with the roughness exponent $\beta = 1/2$. Moreover, we found that the full coverage profile approaches a dimension independent form, thus implying that this approximation ignores interactions. We developed an alternative self-consistent mean field approach that provides a better approximation for the uncovered

fraction, and close estimates for the early time behavior. Additionally, the two approximate approaches combine to give upper and lower bounds for statistical properties such as the coverage, the velocity, and the roughness.

The mean field approach predicts a smooth interface, $\beta = 0$. With increasing the dimension, the roughness exponent decreases from $\beta = 1/2$ at $d = 0$ to $\beta = 0$ at $d \geq d_c$, with d_c the critical dimension [3]. Thus, for sufficiently high dimensions the mean-field behavior should emerge.

The above mean-field theory should allow computation of space-time correlation functions and structure functions. Even more detailed analysis may be possible for one-dimensional substrates. A bigger challenge is to solve the PNG process analytically. Such a solution will undoubtedly illuminate the theoretical understanding of non-equilibrium growth.

PLK acknowledges support from NSF and ARO.

-
- [1] J. Krug and H. Spohn, in *Solids Far From Equilibrium*, edited by C. Godrèche (Cambridge University Press, Cambridge, 1992).
 - [2] P. Meakin, *Phys. Rep.* **235**, 191 (1993).
 - [3] T. Halpin-Healy and Y.-C. Zhang, *Phys. Rep.* **254**, 215 (1995).
 - [4] A.-L. Barabasi and H. E. Stanley, *Fractal Concepts in Surface Growth* (Cambridge University Press, Cambridge, 1995).
 - [5] F. C. Frank, *J. Cryst. Growth* **22**, 233 (1974).
 - [6] D. Kashchiev, *J. Cryst. Growth* **40**, 29 (1977).
 - [7] G. H. Gilmer, *J. Cryst. Growth* **49**, 465 (1980).
 - [8] A. Keller, *Rep. Prog. Phys.* **31**, 623 (1968).
 - [9] D. C. Bassett, *Principles of Polymer Morphology* (Cambridge University Press, Cambridge, 1995).
 - [10] A. N. Kolmogorov, *Bull. Acad. Sci. USSR, Phys. Ser.* **1**, 355 (1937).
 - [11] M. Avrami, *J. Chem. Phys.* **7**, 1103 (1939); **8**, 212 (1940); **9**, 177 (1941).
 - [12] W. A. Johnson and P. A. Mehl, *Trans. AIMME* **135**, 416 (1939)
 - [13] K. Sekimoto, *Physica A* **135**, 328 (1986).
 - [14] K. Sekimoto, *Int. J. Mod. Phys. B* **5**, 1843 (1991).
 - [15] R. M. Bradley and P. N. Strenski, *Phys. Rev. B* **40**, 8967 (1989).
 - [16] E. Ben-Naim and P. L. Krapivsky, *Phys. Rev. E* **54**, 3562 (1996).
 - [17] J. W. Evans, *Rev. Mod. Phys.* **65**, 1281 (1993).
 - [18] M. C. Bartelt and J. W. Evans, *J. Phys. A* **26**, 2743 (1993).
 - [19] T. J. Newman and A. Volmer, *J. Phys. A* **29**, 2285 (1996).
 - [20] C. H. Bennett, M. Büttiker, R. Landauer, and H. Thomas, *J. Stat. Phys.* **24**, 419 (1981).
 - [21] N. Goldenfeld, *J. Phys. A* **17**, 2807 (1984).

- [22] W. van Saarloos and G. H. Gilmer, *Phys. Rev. B* **33**, 4927 (1986).
- [23] J. Krug and H. Spohn, *Europhys. Lett.* **8**, 219 (1989).
- [24] J. Krug, P. Meakin, and T. Halpin-Healy, *Phys. Rev. A* **45**, 638 (1992).
- [25] M. Toda, *J. Phys. Soc. Jpn.* **22**, 431 (1967).
- [26] M. Bramson, *Convergence of Solutions of the Kolmogorov Equation to Travelling Waves* (American Mathematical Society, Providence, R.I., 1983).
- [27] J. D. Murray, *Mathematical Biology* (Springer-Verlag, New York, 1989).
- [28] C. M. Bender and S. A. Orszag, *Advanced Mathematical Methods for Scientists and Engineers* (McGraw-Hill, Singapore, 1984).
- [29] R. D. Armstrong and J. A. Harrison, *J. Electrochem. Soc.* **116**, 328 (1969).
- [30] S. K. Rangarajan, *J. Electroanal. Chem.* **46**, 125 (1973).